Liquid Crystals
Publication details, including instructions for authors and subscription information:
http://www.informaworld.com/smpp/title~content=t713926090

Self-assembled diols: synthesis, structure and dielectric studies

Jessie Lorenzo Chao[a]; Ilja Grebenchtchikov[a]; Robert Kieffer[a]; Zinaida Vakhovskaya[a]; Ute Baumeister[a]; Carsten Tschierske[a]; Horst Kresse[a]
[a] Martin-Luther-Universität Halle-Wittenberg, Institut für Physikalische Chemie, D-06108 Halle, Germany

To cite this Article Chao, Jessie Lorenzo , Grebenchtchikov, Ilja , Kieffer, Robert , Vakhovskaya, Zinaida , Baumeister, Ute , Tschierske, Carsten and Kresse, Horst(2006) 'Self-assembled diols: synthesis, structure and dielectric studies', Liquid Crystals, 33: 10, 1095 — 1102
To link to this Article: DOI: 10.1080/02678290600732212
URL: http://dx.doi.org/10.1080/02678290600732212

Liquid Crystals, Vol. 33, No. 10, October 2006, 1095–1102

Taylor & Francis
Taylor & Francis Group

Self-assembled diols: synthesis, structure and dielectric studies

JESSIE LORENZO CHAO, ILJA GREBENCHTCHIKOV, ROBERT KIEFFER, ZINAIDA VAKHOVSKAYA, UTE BAUMEISTER, CARSTEN TSCHIERSKE and HORST KRESSE*

Martin-Luther-Universität Halle-Wittenberg, Institut für Physikalische Chemie, Mühlpforte 1, D-06108 Halle, Germany

(*Received 16 December 2005; accepted 6 March 2006*)

In single-, double-, and triple-chain amphiphilic diols the CONH group was replaced by $CON(CH_3)$ in order to reduce the number of proton donor groups available for intermolecular hydrogen bonding. The resulting three new liquid crystalline diols were studied by DSC, X-ray and dielectric measurements, and show the mesophases SmA, Col_{H2} or Cub_{I2}, depending on the number of decyloxy groups in the hydrophobic part of the molecule. The process of self-assembly to different liquid crystalline phases is well seen in the dielectric spectrum and details of this process are discussed together with results from the X-ray measurements. All the compounds show a high frequency dielectric absorption caused by the dynamics of the network of hydrogen bonds. An additional low frequency process related to the internal dynamics of the columns is seen only in the columnar phase.

1. Introduction

Simple amphiphilic diols consisting of hydrophobic alkyl chains and at least two hydroxyl groups as the hydrophilic unit form amphotrophic liquid crystalline phases [1–5]. The driving force for the self-assembly are the nano-scale segregation of polar and lipophilic units and the tendency to build up a network of hydrogen bonds. Earlier investigations have shown that the dielectric method is a useful tool for studying details of the self-organization process [5–10]. In the amphiphilic diols reported earlier the number and the length of the lipophilic chains were changed systematically and the phase sequence $SmA–Cub_{V2}–Col_{H2}–Cub_{I2}$ was found with increasing size of the lipophilic units [6]. For synthetic reasons the interconnection of the lipophilic molecular segments with the hydrophilic 1,2-propanediol unit was achieved using a CONH group. There remains the question about the importance of the CONH group as proton donor group for the self-organization in general and specially for the low frequency dynamics in the columnar phase. This process is difficult to separate from the conductivity and double layer effects of the diols. Therefore the CONH group of earlier published compounds [6] was replaced by $CON(CH_3)$. This substitution also changes the lateral interaction and the shape of the molecules with respect to the non-methylated compounds.

*Corresponding author. Email: horst.kresse@chemie.uni-halle.de

2. Synthesis

The synthesis of compounds **1**–**3** with different numbers of dodecyloxy groups is shown in scheme 1.

2.1. *N-(2,3-Dihydroxypropyl)- N-methyl-4-dodecyloxybenzamide (1)*

1.5 g (5 mmol) 4-dodecyloxybenzoic acid was dissolved in 50 ml dry THF and 1 g (5 mmol) DCC was added at 0°C. After 15 min the mixture was heated to room temperature and 1 g (5.5 mmol) pentafluorophenol was added. The mixture was stirred for 24 h, 1.05 g (10 mmol) 3-methylamino-1,2-propandiol was added and again the mixture was stirred for 24 h. After filtration the residue was washed with $CHCl_3$. The solvent was evaporated in vacuum, and the residue was purified by column chromatography on silica gel with $CHCl_3$/MeOH as eluant and crystallized from methanol; yield 0.9 g (48%). ^{1}H NMR ($CDCl_3$, ppm): δ=7.37 (d, J=8.7 Hz, 2H, H-ar), 6.87 (d, J=8.7 Hz, 2H, H-ar), 3.96–3.93 (m, 3H, CH_2O, C**H**OH), 3.62–3.57 (m, 4H, NCH_2, C**H**$_2$OH), 3.5–3.2 (bs, 2H, OH), 3.08 (s, 3H, N-CH_3), 1.79–1.72 (m, 2H, C**H**$_2$–CH_2O), 1.46–1.39 (m, 2H, C**H**$_2$–CH_2–CH_2O), 1.32–1.24 (m, 16H, CH_2), 0.86 (t, J=6.7 Hz, 3H, CH_3).

2.2. *N-(2,3-Dihydroxypropyl)- N-methyl-3,4-didodecyloxybenzamide (2)*

Compound **2** was prepared according to the procedure given above with 1.5 g (3 mmol) 3,4-didodecyloxybenzoic

Liquid Crystals
ISSN 0267-8292 print/ISSN 1366-5855 online © 2006 Taylor & Francis
http://www.tandf.co.uk/journals
DOI: 10.1080/02678290600732212

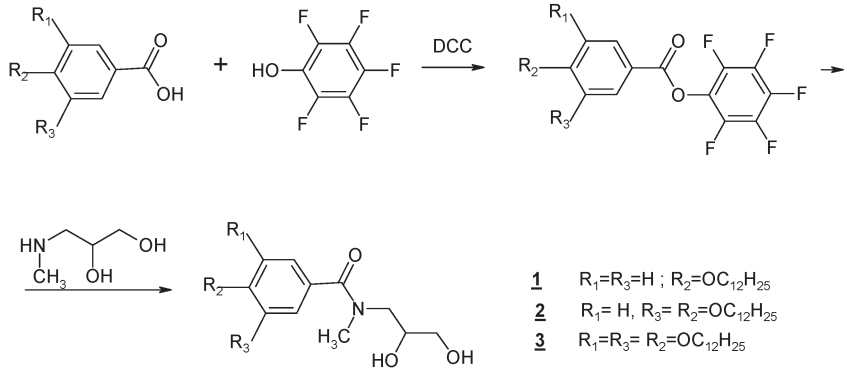

Scheme 1. Synthesis of compounds **1**–**3**.

acid as starting material. The yield was 0.86 g (52 %). ^{1}H NMR ($CDCl_3$, ppm): δ=6.96 (m, 2H, H-ar), 6.83 (d, J=8.5 Hz, 1H, H-ar), 3.99 (t, J=6.6 Hz, 2H, CH_2O), 3.98 (t, J=6.6 Hz, 2H, CH_2O), 3.95–3.92 (m, 1H, C**H**OH), 3.66–3.59 (m, 4H, NCH_2, C**H**$_2$OH), 3.09 (s, 3H, N–CH_3), 2.82 (bs, 2H, OH), 1.84–1.76 (m, 4H, C**H**$_2$–CH_2O), 1.48–1.41 (m, 4H, C**H**$_2$–CH_2–CH_2O), 1.35–1.25 (m, 32H, CH_2), 0.86 (t, J=6.9 Hz, 6H, CH_3).

2.3. *N-(2,3-Dihydroxypropyl)- N-methyl-2,3,4-tridodecyloxybenzamide (3)*

Compound **3** was prepared in an analogous way from 2 g (4.5 mmol) 3,4,5-tridodecyloxybenzoic acid. The yield was 1.5 g (48%). ^{1}H NMR ($CDCl_3$, ppm): δ=6.59 (s, 2H, H-ar), 3.96–3.93 (m, 7H, CH_2O, C**H**OH), 3.64–3.60 (m, 4H, NCH_2, C**H**$_2$OH), 3.07 (s, 3H, N–CH_3), 2.79 (bs, 2H, OH), 1.81–1.68 (m, 6H, C**H**$_2$–CH_2O), 1.44–1.41 (m, 6H, C**H**$_2$–CH_2–CH_2O), 1.28–1.25 (m, 48H, CH_2), 0.86 (t, J=6.8 Hz, 9H, CH_3).

3. Phase transitions

The phase transition temperatures were estimated from the maxima of the DSC traces using a cooling rate of 3 K min^{-1}. The samples were heated to 400 K in order to remove water traces and were immediately sealed. The melting temperatures were taken from the first heating run.

The clearing temperatures of compounds **1**–**3** (table 1) are about 60 K lower than those of the analogous compounds with a CONH linking unit instead of the $CONCH_3$ unit [6]. The data of the latter are included in table 1 and indicated by *1–3* in italic letters. This decrease is due to the reduced number of H-donor groups available for hydrogen bonding and the change of the lateral interaction. As in the case of the CONH-linked compounds with the same chain length ($OC_{12}H_{25}$), the single chain compounds show a SmA phase and the double-chain compounds a Col_{H2} phase. Only for the triple-chain compounds a different phase is sequence observed. Whereas the CONH-linked compound has only a micellar cubic phase (Cub_{I2}/*Pm*3*n*) over the whole mesomorphic temperature range, an additional Col_{H2} phase was found below the Cub_{I2} phase of compound **3**. This should be mainly due to the size of the CH_3 group which enlarges the polar part of the amphiphilic molecule and hence reduces the interface curvature and allows the formation of a Col_{H2} phase at reduced temperature. However, for the Cub_{I2}/I transition of substance **3** no clear calorimetric effect was

Table 1. Phase transition temperatures in K, transition enthalpies in kJ mol^{-1} (values in brackets) and phases of the compounds **1**–**3**. For comparison the transition temperatures of the related compounds with the CONH group *1–3* according to [6] are given in italics.

Sample	Cr		Col_{H2}		Cub_{I2}		SmA		I
1	•	325	—	—	—	—	•	353 (1.19)	•
1	.	*362*	—	—	—	—	.	*405*	.
2	•	321	•	361 (0.32)	—	—	—	—	•
2	.	*371*	.	*421*	—	—	—	—	.
3	•	296	•	307 (1.9)	•	327 (—)	—	—	•
3	.	*342*	—	—	.	*399*	—	—	.

detected. This might be due to the supercooling/overheating of this phase transition. In addition it could be quite slow so that the peak is smeared out over a rather broad temperature range and therefore cannot be detected in the DSC curves.

4. X-ray investigations

X-ray investigations on powder-like samples were carried out with a Guinier film camera (Huber). The samples were held in glass capillaries (diam. 1 mm) in a temperature-controlled heating stage (measuring conditions: quartz-monochromatized CuK_α radiation, 30 to 60 min exposure time, calibration with the powder pattern of $Pb(NO_3)_2$). Alignment of samples on a glass plate was achieved by slow cooling of a small droplet of the sample on the temperature-controlled heating stage, and took place at the sample–glass or sample–air interface giving domains that are fibre-like disordered around an axis perpendicular to the interface. The diffraction patterns were recorded with an area detector (HI-STAR, Siemens).

The layer spacing of compound **1** obtained by the Guinier method decreases with increasing temperature from 3.9 nm at 313 K to 3.6 nm at 353 K. The two-dimensional X-ray patterns of an aligned sample of compound **2** proved the liquid crystalline phase to be a Col_H one (figure 1). The hexagonal lattice parameter was determined from calibrated Guinier powder patterns and varies from $a=3.9$ nm at 358 K to 4.0 nm at 343 K on cooling. It should be noted that the small angle range of the 2D X-ray pattern of the isotropic liquid shows an intense scattering at θ values near that of the 10 reflection in the Col_H phase, with full width at half-maximum of about 0.3° in θ, figure 1 (*b*). The intensity of this pattern in the isotropic phase remains nearly constant on heating up to 373 K.

The Guinier film pattern of the columnar phase of compound **3** shows three reflections with *d*-values in the ratio of $1 : 1/\sqrt{3} : 1/2$ and can also be assigned as Col_H with $a_{hex}=4.0$ nm at 303 K. In order to denote that the structure consists of inverse micelles the subscript 2 was added to Col_H. The optically isotropic high temperature phase causes Bragg reflections in the small angle range to suffer from strong splitting according to orientational effects, which is typical for a cubic phase. A unique indexing of the reflections was not possible because of these effects.

5. Dielectric measurements

The samples were heated to 393 K and filled after a waiting time of about 20 min in the calibrated measuring capacitor ($d=0.05$ mm). Dielectric measurements were made during cooling using the Solartron–Schlumberger Impedance Analyzer Si 1260. The samples could not be oriented. Experimental details are given elsewhere [11]. The raw data were fitted to two Cole–Cole mechanisms [12]

$$\varepsilon^* = \varepsilon_2 + \frac{\varepsilon_0 - \varepsilon_1}{1 + (j\omega\tau_1)^{1-\alpha_1}} + \frac{\varepsilon_1 - \varepsilon_2}{1 + (j\omega\tau_2)^{1-\alpha_2}} - \frac{jA}{f^M} + \frac{B}{f^N} \quad (1)$$

with the limiting values ε_i of the dielectric permittivity and the corresponding relaxation times τ_i with $\omega=2\pi f$ (f=frequency), α_i=Cole–Cole distribution parameters, the conductivity term A as well as M, B and N as further fit parameters responsible for the slope of conductivity and capacity of the double layer were calculated.

For the calculation of the specific conductivity, data for the dielectric loss ε'' between 100 and 1000 were fitted to the fourth term in equation (1) under the condition $M=1$ [10]. The condition $M=1$ was also nearly fulfilled with M as open parameter because M fluctuates between 0.985 and 1.000. The specific

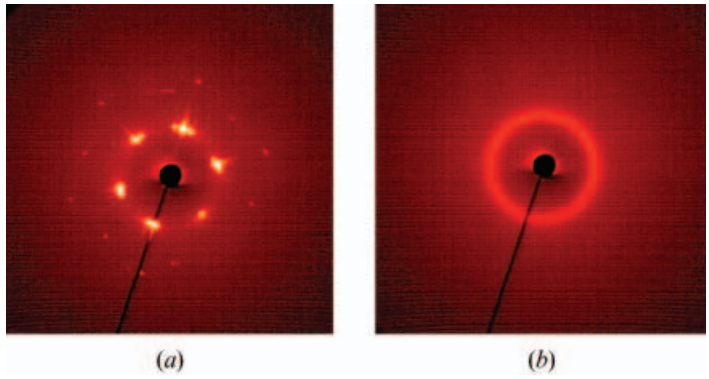

Figure 1. Small angle range of the X-ray patterns of **2**: (*a*) for an aligned sample at 353 K on cooling; (*b*) for the isotropic liquid at 361 K just before the transition from the isotropic liquid phase to the columnar phase.

conductivity κ was calculated from the A-parameter according to

$$\kappa = A 2\pi 8.85 \times 10^{-12}\,\mathrm{S\,m^{-1}}\,[12]. \quad (2)$$

The error in the static dielectric permittivity ε_0 obtained from a fit of the raw data (see figure 2) to equation (1) in the SmA and Cub_{I2} phases is about 1% at low and 2% at high temperatures. The fitted ε_1 and τ_1 parameters show an uncertainty of about 2% and 20%, respectively, and the specific conductivity one of 1%. The static dielectric permittivity ε_0 in the Col_{H2} state of substance **2** reaches a maximum error of 20%. This higher error results from the superposition of electric double layer and conductivity with the dielectric absorption range. The actual errors in the dielectric permittivities (but not in the relaxation times) measured in the anisotropic phases, SmA and Col_{H2}, are bigger because the orientation of the samples is unknown.

Figures 2 and 3 present the complex dielectric function $\varepsilon^* = \varepsilon' - j\varepsilon''$ of compound **2** in the isotropic (I) and the Col_{H2} phases as well as fits to equation (1). The contributions of conductivity and electric double layer dominate the spectrum at low frequencies and high temperatures. The data obtained in the isotropic phase could be well fitted with the limiting dielectric permittivity ε_1 and the last two terms in equation (1) as shown in figure 2. In the columnar phase, a good fit was only possible under the assumption of an additional low frequency absorption, which reduces the dielectric function from ε_0 to ε_1. This process is not visible in the isotropic state. The contribution of the double layer is indicated by a line in figure 3 in order to see the low frequency absorption better. The error of all fitted parameters related to this process (ε_0, f_{R1}, α_1) is large due to the superposition with double layer and conductivity. The high frequency dispersion reduces the dielectric permittivity from ε_1 to ε_2 and exhibits a Cole–Cole distribution parameter of 0.4. This process also occurs in the isotropic state at the experimental limit. Important parameters of the fit are presented in the figures 4–6.

The limits of the dielectric function, ε_0 and ε_1, given in figure 4, show a strong increase at the I/Col_{H2} transition. This effect results from the self-assembly of the molecules into columns. Due to the appearance of the additional low frequency process in the Col_{H2} phase with the limit ε_0, the 'static' dielectric permittivity in the isotropic phase was denoted ε_1 in order to use the same

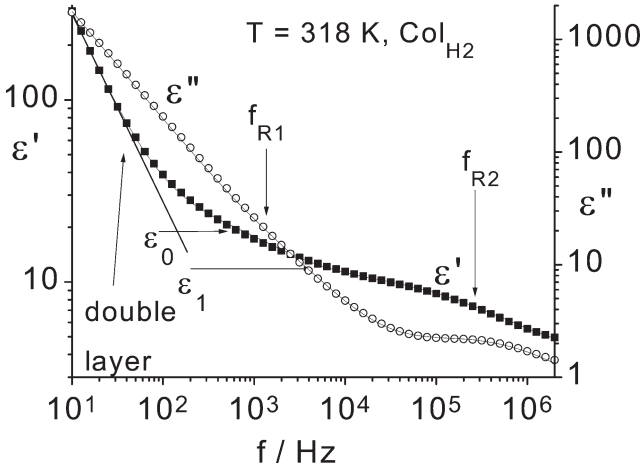

Figure 3. Complex dielectric function of compound **2** in the Col_{H2} phase.

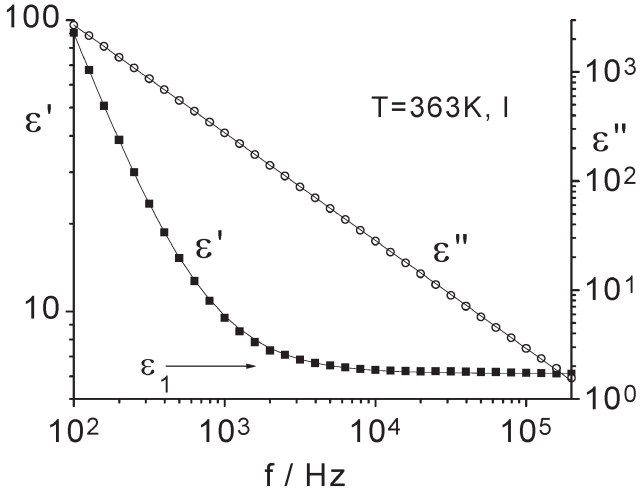

Figure 2. Complex dielectric function of compound **2** in the isotropic phase.

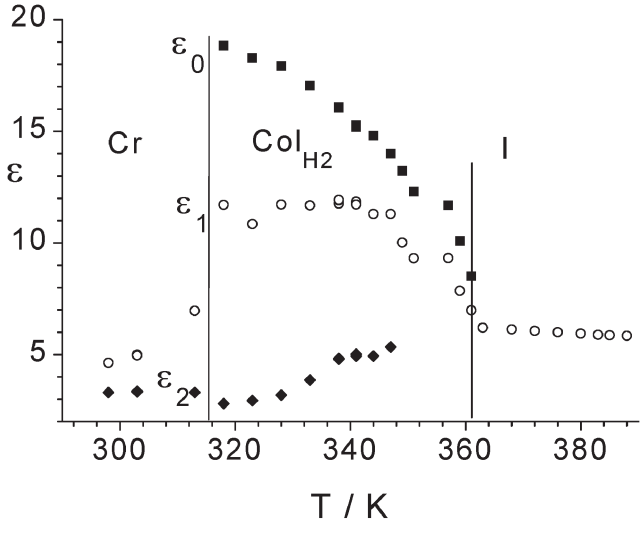

Figure 4. Limits of the dielectric permittivity of compound **2** as obtained from the fit.

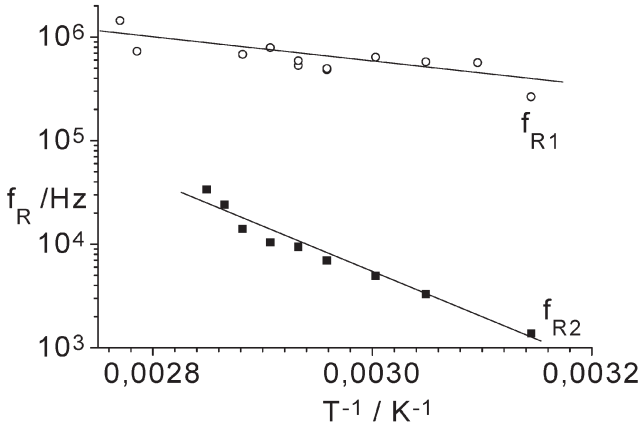

Figure 5. Relaxation frequencies of compound **2** versus the reciprocal temperature.

symbols for the same mechanisms. Furthermore, the slope of the dielectric permittivity in the isotropic phase ($d\varepsilon/dT$) amounts to -0.013 ($\varepsilon=6.0$). This value agrees well with that of chlorobenzene, ($d\varepsilon/dT$)$=-0.0133$ ($\varepsilon=5.7$) [13], and proves that it should be either related to non-associated molecules or to thermally very stable associates. An intermediate case can be excluded because an increasing dissociation would also increase the dielectric permittivity with temperature due to the decomposition of the associates as discussed later. The two relaxation processes show large differences in the activation energies: $E_1=(83\pm6)\,\mathrm{kJ\,mol^{-1}}$ and $E_2=(23\pm6)\,\mathrm{kJ\,mol^{-1}}$ (figure 5). The specific conductivity given in figure 6 increases slightly at the I/Col_{H2} transition. This behaviour indicates a more parallel orientation of the columns to the measuring electric field [10, 14].

Experimental data at $T=313$ K and the fitted limits of the dielectric permittivities of compound **1** are presented

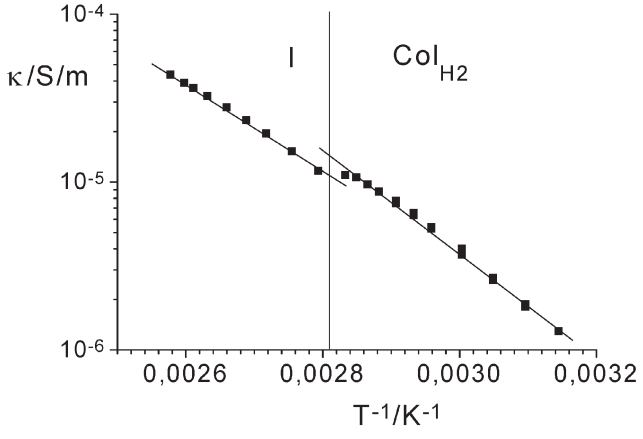

Figure 6. Specific conductivity of compound **2** versus the reciprocal temperature.

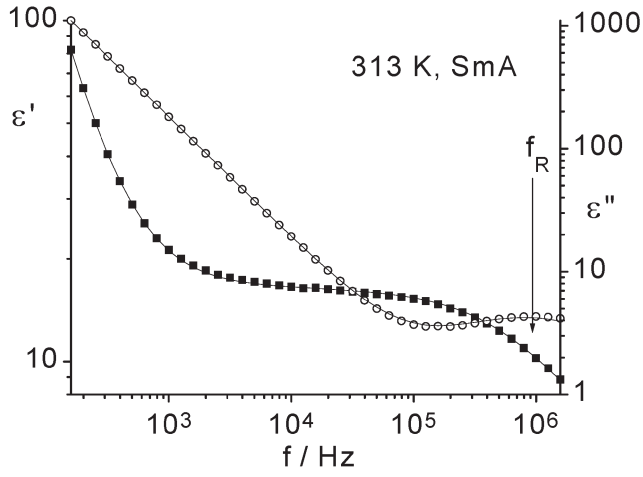

Figure 7. Row data and fits of compound **1** in the SmA phase.

in figures 7 and 8. Only a high frequency relaxation range was detected, which could be well separated at lower temperatures (see figure 7). Thus, at $T=313$ K ($1/T=0{,}00319\,\mathrm{K^{-1}}$) a relaxation frequency of 1 MHz was obtained, which almost agrees with the data of compound **2** shown in figure 5. The specific conductivity (not shown) and ε_0 (see figure 8) increase only very slightly at the I/SmA transition, probably resulting from the statistically oriented net of hydrogen bonds [10].

Compound **3** is very interesting because it forms two mesophases. As in the case of compound **2** the limit of the low frequency process in the Col_{H2} phase was named ε_0. Consequently, the 'static' dielectric permittivity in the isotropic and cubic phase was termed ε_1. ε_1 shows a step at the Cub_{I2}/I transition as typical behaviour [10], as can be seen in the inset of figure 9, which allowed us to fix the transition temperature given

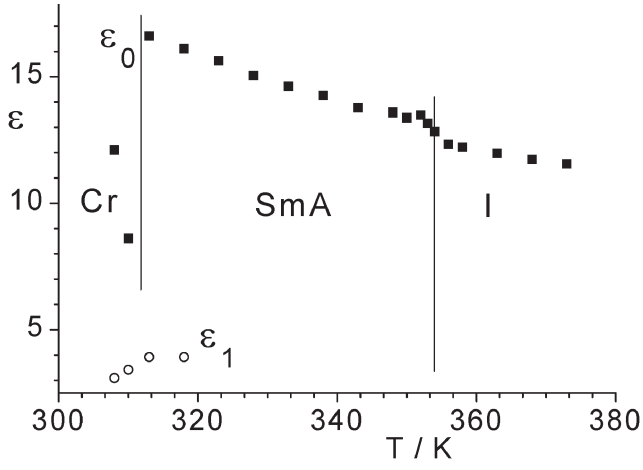

Figure 8. Limits of the dielectric permittivities of compound **1**.

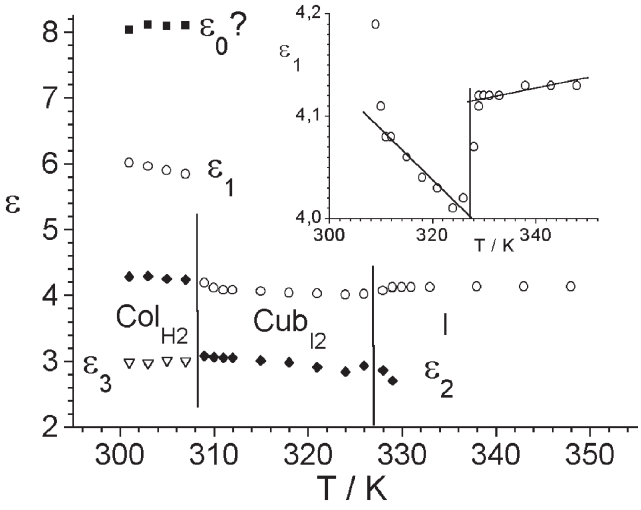

Figure 9. Limits of the dielectric permittivity of compound **3**.

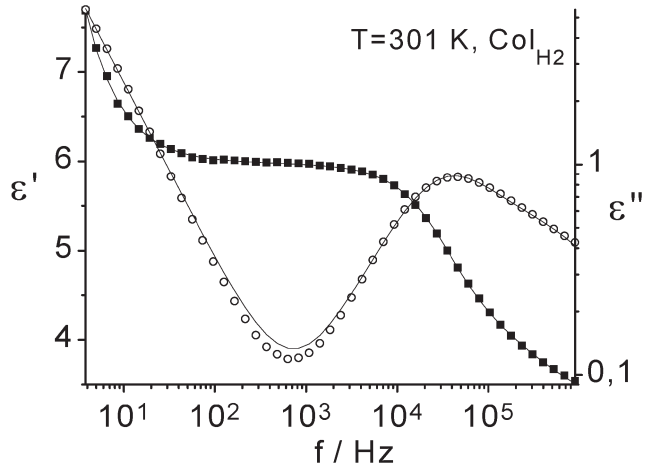

Figure 11. Complex dielectric function of compound **3** in the columnar phase.

in table 1. ε_1 also strongly increases at the transition into the columnar modification. Furthermore, the slope of ε_1 in the isotropic state $d\varepsilon/dT$ is positive and was fitted to $(7 \pm 2) \times 10^{-4}\,K^{-1}$. The specific conductivity shown in figure 10 decreases by one decade at the I/Cub_{I2} transition and increases again at the transition into the Col_{H2} state [7].

The raw data of the complex dielectric function for compound **3**, presented in figure 11, show an asymmetric high frequency process in the columnar phase. Two Cole–Cole processes have been used to describe the asymmetric absorption. A Havriliak–Negami fit [12] can also be applied. In our case one cannot distinguish between these two interpretations. Therefore the separation into two mechanisms should not be over-interpreted. Activation energies of $43 \pm 5\,kJ\,mol^{-1}$ (Col_{H2}) and $38 \pm 3\,kJ\,mol^{-1}$ (Cub_{I2}) have been calculated for the high frequency mechanism 2 indicated by open circles. A second problem is not shown in figure 11, namely the appearance of a low frequency process with the limit ε_0 as discussed for compound **2**. The fit of the complex dielectric function at low frequencies was much better assuming an additional low frequency absorption at about 3 Hz, but the statistical uncertainty of all parameters calculated in this case is about 60%. Thus the actual existence of this relaxation process must be open to question. A question-mark is therefore added to the related parameters ε_0 in figure 9 and the relaxation frequencies f_{R1} in figure 12.

6. Discussion

First the nature of the observed relaxation processes will be discussed. All the compounds show an absorption

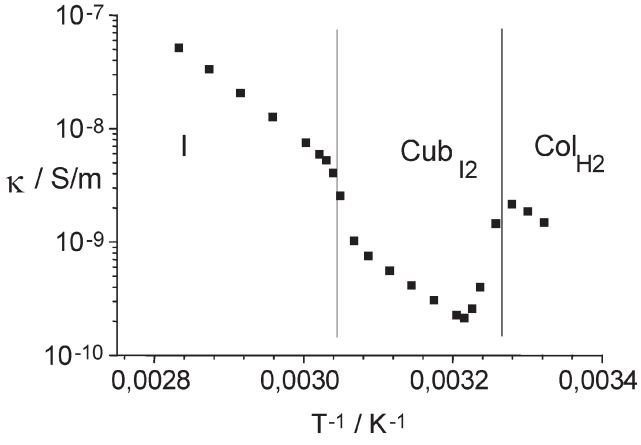

Figure 10. Specific conductivity of compound **3** versus the reciprocal temperature.

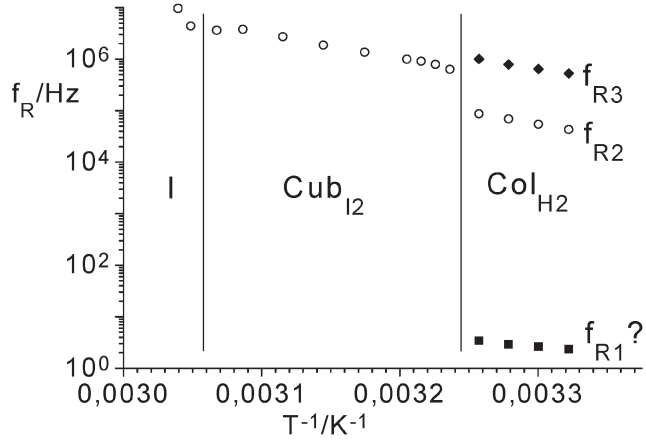

Figure 12. Relaxation frequencies of compound **3** in the columnar phase.

with the relaxation frequency 1 MHz at about 325 K. Therefore we relate this process to the dynamics of the system of hydrogen bonds. It is also possible that this process contains contributions from local motions, for example the reorientation of the $CON(CH_3)$ groups. We assign the low frequency process clearly seen only in the Col_{H2} phase of compound **2** to internal dynamics within the columns [10]. The idea of a rotating dipole [7] can be excluded, because this relaxation range appears in a compound in which the hydrogen of the CONH group is substituted by the CH_3 group, which is unable to take part in the network of hydrogen bonds. Consequently, we must explain the low frequency relaxation in the classical way by an elastic deformation of the columns due to interaction with the measuring electric field.

The interesting process of self assembly of the three different compounds will now be considered. Compound **1** shows a slope $d\varepsilon/dT = -0{,}046\,K^{-1}$ in the isotropic phase (figure 8). This is a behaviour which can be expected for isolated molecules with a static dielectric permittivity of 12. Hence we can assume that only the double layers of the SmA phase are destroyed at the clearing temperature and single molecules appear.

Compound **2** shows only a columnar phase. As in published structure models [5] we can assume that the wedge-shaped diole molecules associate by a net of hydrogen bonds located in the interior of the columns, the hydrocarbon chains having a liquid-like organization around the core of the columns. Such an inverted columnar phase is commonly asigned as Col_{H2}. An estimate of 6.5 for the average number n of molecules arranged in the cross-section of a column can be calculated according to equation (3) from the hexagonal lattice parameter $a = 4.0$ nm (at 343 K), assuming an average distance $h = 0.45$ nm for the molecules along the columnar axis and an approximate density $\rho \approx 1\,g\,cm^{-3}$ ($M = 577.9\,g\,mol^{-1}$, N_A = Avogadro constant, see [5] for details).

$$n = \left(a^2/2\right)\sqrt{3}h(N_A/M)\rho. \qquad (3)$$

The dielectric behaviour changes completely at the transition Col_{H2}/I as can be seen in figures 4 and 5. On one hand, the relatively narrow and intense scattering in the small angle range of the X-ray pattern at 361 K should result from a short range ordered arrangement in the isotropic state. The θ value for the intensity maximum of this scattering agrees well with that of the 1 0 reflection in the columnar phase (see figure 1) with a d-value of 3.5 nm corresponding to $a_{hex} = 4.0$ nm. On the other hand, the length of the molecular long axis is only 2.9 nm, measured from CPK models in the most extended conformation, so the scattering cannot arise from the monomers. A calculation of the correlation lengths for corresponding associates would require that high resolution small angle X-ray measurements be undertaken. In a qualitative way, however, one can assume that the cylindrical micelles are stable in the temperature range investigated, including the isotropic phase, and the dielectric results reflect only the self-assembly of the cylindrical micelles to the hexagonal superstructure.

The behaviour of the specific conductivity of the triple-chain compound **3** closely resembles that of its CONH derivative with 8 C-atoms in the chains, which has the same Col_{H2}–Cub_{I2} phase sequence [5]. The low temperature Col_{H2} phase of compound **3** with a hexagonal lattice parameter $a = 4.0$ nm (at $T = 303$ K) is built of columns containing on average 4.9 molecules in their cross-section according to equation (3), assuming the same values for h and ρ as in case of compound **2**. These measures are in a very good agreement with the model for other Col_{H2} phases of wedge-shaped compounds, especially with that for the three-chain polyhydroxy amphiphiles mentioned earlier [5].

The decrease of the specific electric conductivity at the phase transition Col_{H2}/Cub is a clear indication of the formation of a micellar cubic phase asigned Cub_{I2} with an inverse micelle structure. Most probably, a similar model as given earlier for the cubic phase above a Col_{H2} phase in [5] may be applied and the closed micelles forming the cubic phase are fragments of the columns in the Col_{H2} phase.

The transition Cub_{I2}/I takes place in two steps: (1) the destruction of the cubic lattice formed by micelles at the phase transition temperature, and (2) the further destruction of the micelles with increasing temperature. The latter process is responsible for the positive slope of ε versus T shown in figure 9, because the longitudinal dipole moments compensate each other in the spherical or nearly spherical micelles. Thus, the increasing monomer content with increasing temperature increases the effective dipole moment per volume unit.

Acknowledgements

The authors are indebted for financial support to the DFG (Graduiertenkolleg 894).

References

[1] D. Blunk, K. Praefke, V. Vill. In *Handbook of Liquid Crystals,* Vol. 3, D. Demus, J. Goodby, G.W. Gray, H-W. Spiess (Eds), pp. 305–340 (1998).

[2] D.M.P. Mingos (Ed.). *Supramolecular Assembly via Hydrogen Bond, I and II,* Springer, Berlin (2004).

[3] C. Tschierske, *Prog. Polym. Sci.*, **21**, 775 (1996); C. Tschierske, *Curr. Opin. Colloid Interf. Sci.*, **7**, 355 (2002).
[4] C. Tschierske. *J. mater. Chem.*, **8**, 1485 (1998).
[5] K. Borisch, S. Diele, P. Göring, H. Kresse, C. Tschierske, *Angew. Chem.*, **109**, 2188 (1997); *Angew. Chem. int. Ed. Engl.*, **36**, 2087 (1997) and references therein.
[6] K. Borisch, S. Diele, P. Göring, H. Kresse, C. Tschierske. *J. mater. Chem.*, **8**, 529 (1998).
[7] H. Kresse, H. Schmalfuss, B. Gestblom, K. Borisch, C. Tschierske. *Liq. Cryst.*, **23**, 891 (1997).
[8] H. Schmalfuss, K. Borisch, C. Tschierske, H. Kresse. *Mol. Cryst. liq. Cryst.*, **331**, 129 (1999).
[9] H. Kresse. *Polym. Repr.*, **40**, 1107 (1999).
[10] J. Lorenzo Chao, Z. Vakhovskaya, I. Grebenchtchikov, C. Tschierske, H. Kresse. *Liq. Cryst.*, **32**, 1295 (2006).
[11] H. Kresse, H. Schlacken, U. Dunemann, M.W. Schröder, G. Pelzl. *Liq. Cryst.*, **29**, 1509 (2002).
[12] A. Schönhals, F. Kremer. In *Broadband Dielectric Spectroscopy*, F. Kremer, A. Schönhals (Eds), Springer, Berlin, 60 (2003).
[13] C.D. Hodgman, R.C. Weast, R.S. Shankland, S.M. Selby. *Handbook of Chemistry and Physics*, 2611, The Chemical Rubber Publ. Co. Cleveland, Ohio (1962).
[14] R. Germer, F. Giesselmann, P. Zugenmaier, C. Tschierske. *Mol. Cryst. liq. Cryst.*, **331**, 643 (1999).